

## Preface

Diagnostic imaging of the heart has a long tradition in Germany, starting over a century ago with the discovery of Wilhelm Conrad Röntgen, which forms the basis for all radiographic techniques of cardiac imaging. Another milestone was the development of cardiac ultrasonography, which began in Germany during the 1940s and was perfected by Edler and Hertz, who recorded the first tracings of the heart based on ultrasound reflection. Professor Sven Effert introduced the method in Germany and was instrumental in gaining national and international recognition. Other key milestones were the development of computed tomography and magnetic resonance imaging.

The creation of this book was motivated by a desire to combine expert knowledge from the two medical specialties of cardiology and radiology, which have been responsible for tremendous advances in the diagnosis of heart diseases.

A third essential field in developing cardiac imaging is medical physics, which has fostered fascinating developments based on work that gained several Nobel Prize awards to physicists. Equally essential is the sectional imaging triad of echocardiography, computed tomography, and magnetic resonance imaging, whose basic physical principles have contributed to the current worldwide high level of development through systematic advances in medical technology.

Against this background of innovations and advances, it has been a genuine pleasure for the editors and authors to compile a synopsis of modern cardiac imaging and summarize the advances in this field, which are most clearly reflected in sectional imaging modalities. The new role of nuclear medicine imaging (PET-CT) is also considered in this context. Despite the profound insights that modern techniques have provided into the pathological anatomy of the heart and especially its function, conventional radiographs are far from obsolete and are available for almost every patient. Radiographs should not be ordered indiscriminately, however; this relatively low-cost and well-tolerated study should be applied critically and selectively. Recognizing that decades of experience in the analysis of chest radiographs should be fully exploited, we open this book by reviewing the basic aspects of conventional radiography.

It takes more than a detailed knowledge of sectional imaging studies to maintain high medical standards and obtain certification. It is also necessary to have well-planned organizational and communication structures within and among the different specialties as well as a command of current and traditional knowledge in order to achieve a true “state of the art status.”

*Manfred Thelen  
Raimund Erbel  
Karl-Friedrich Kreitner  
Joerg Barkhausen*

## Acknowledgments

Even in the age of internet-based media, the printed page still has an undisputed role in medical education. Information technology is less a competitor of books than a tool to enhance the visual impact of a book and make its contents more accessible to the reader.

*Cardiac Imaging* takes full advantage of these modern capabilities, particularly in its illustrations, which were processed with the aid of digital image processing techniques.

This has all been made possible by the ambitious and dedicated support of Thieme Medical Publishers under the direction of Dr. Albert Hauff and his colleagues. The editors and authors express special thanks to the project manager of this book, Ms. Susanne Huiss, and to Ms. Martina Dörsam, who was responsible for production of the book. We are also grateful to Dr. Christian Urbanowicz, who outlined the cost parameters for the book so that it could be presented in its current form.

The editors and authors thank all of our colleagues at hospitals and other institutions who helped compile the superb illustrations for this book. We are grateful to the entire staff at the Echocardiography Laboratory of the Department of Cardi-

ology, University of Essen, and especially to Ms. Christiane Plato, the medical technologist at that institution. We extend special thanks to our colleagues Björn Plicht, Alexander Lind, Philip Kahlert, and Dirk Böse for their help in compiling the illustrations.

Dr. Peter Hunold, Dr. Thomas Schlosser, Ms. Lena Schäfer, and Mr. Kai Reiter of the Department of Diagnostic and Interventional Radiology, Essen University Hospital, were instrumental in the preparation of this book, and their help is gratefully acknowledged.

We express thanks to Ms. Ine Mayer and Ms. Josefine Kestel, radiology technologists at the Department of Diagnostic and Interventional Radiology university hospital Mainz, and we thank our photographer, Ms. Anne Marie Keuchel, for her conscientious and dedicated work.

*Manfred Thelen  
Raimund Erbel  
Karl-Friedrich Kreitner  
Joerg Barkhausen*

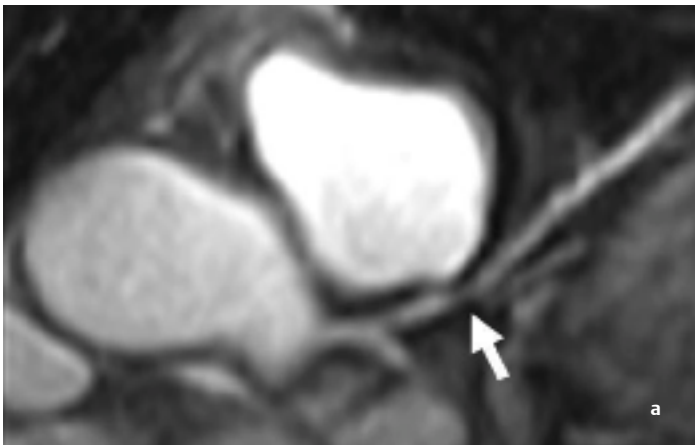
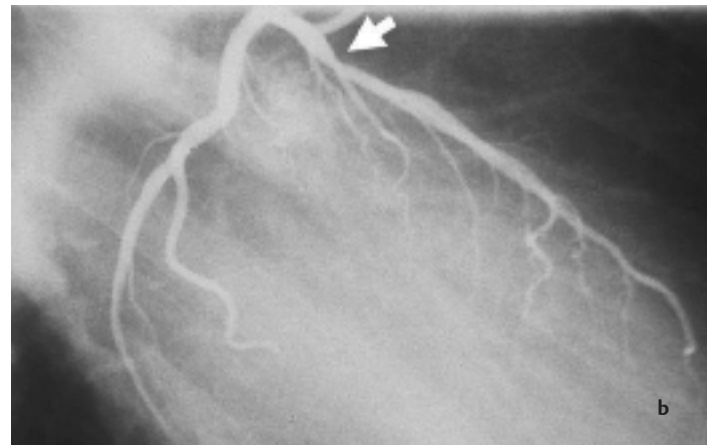


**Fig. 6.39 a** Unenhanced free-breathing MRCA demonstrates a stenosis in the proximal portion of the left coronary artery (arrow).



**b** Finding at the same location on conventional angiography (arrow) (with kind permission of T. Sommer, Bonn University Hospital).

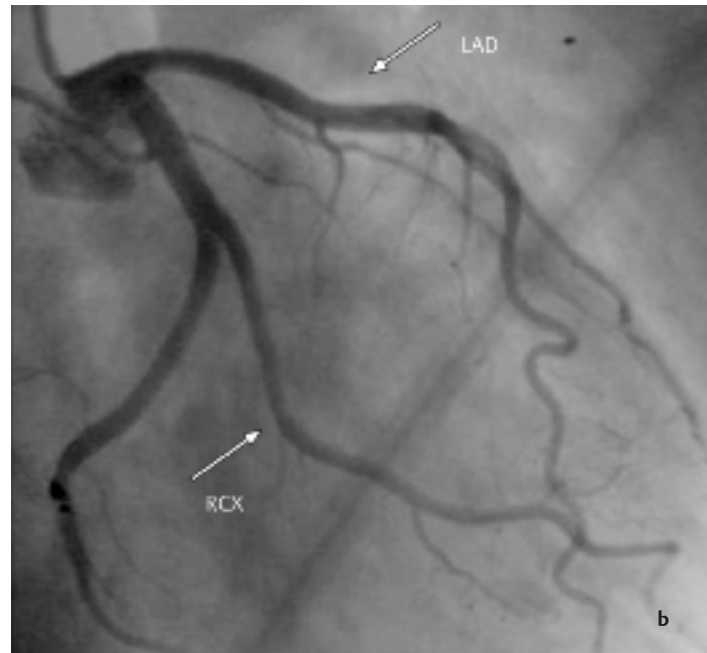


**Fig. 6.40 a, b** MRCA of the left coronary system in a patient with inflammatory signs and suspected Mediterranean fever shows no apparent abnormalities (a). Conventional angiography (b) confirms this finding (with kind permission of T. Ibrahim and R. M. Botner, Technical University of Munich).

### Kawasaki Disease

Kawasaki disease is a generalized vasculitis of unknown etiology that occurs in small children and may eventually give rise to coronary vascular aneurysms. Subsequent thrombosis of these aneurysms and a reduction in blood flow may lead to myocardial infarction. The aneurysms often reach considerable size, and most are easily detected by MRCA.

## Magnetic Resonance Angiography of the Great Vessels

K.-F. Kreitner

Although MRI has been used since its introduction in clinical practice for the investigation of flow effects, the development of clinically useful MR angiography techniques (MRA) did not begin until the mid-1980s. The first techniques to be developed were time-of-flight angiography and phase-contrast angiography. Used without intravenous contrast agents, they were the

first techniques that permitted the selective visualization of flowing blood, making it possible to image the interior of vessels. However, they did not reach any clinical significance in the diagnosis of intrathoracic vascular diseases, because the intraluminal signal in both techniques is dependent on complex flow effects. Furthermore, respiratory movements and cardiac pulsations in the chest lead to motion artifacts, and the air-filled lung tissue induces susceptibility artifacts.

With advances in gradient technology, T1-weighted 3D sequences were developed that made it possible to acquire a complete dataset in less than 30s. These sequences could be acquired during a single breath hold. The heavy saturation of flowing spins requires the use of an effective T1-shortening contrast agent to produce an intraluminal signal that is very bright in relation to the background.<sup>138–141</sup> These enhanced intraluminal signals are virtually independent of flow phenomena, making contrast-enhanced MRA somewhat similar to digital subtraction angiography (**Fig. 6.41**).



**Fig. 6.41** Aneurysm of the ascending aorta in a 65-year-old man. Optimally timed MRA basically limits intravascular enhancement to the aorta and its side branches.

## ■ Basic Technical Principles

### Scanner Hardware and Software

Although MRA of the great thoracic vessels can be performed successfully at 1.0T, 1.5T is considered the standard field strength.<sup>138,139,142</sup> Increasingly, 3.0-T magnets are becoming available for routine clinical imaging, and their use is currently being optimized for thoracic MRA.<sup>143,144</sup>

The speed of an imaging sequence mainly depends on the performance of the gradient system. To achieve short acquisition times, it must be possible to produce magnetic field gradients of very high amplitude that can be switched rapidly on and off. Manufacturers' specifications for maximum amplitudes range from 30 to 45 mT/m with rise times ranging between 100 and 200 mT/m/ms and a maximum field of view (FOV) between 40 and 53 cm.<sup>145–147</sup> Another important parameter is the number of receiver channels that are available to receive the signal from a single surface coil element. While four receiver channels are sufficient for conventional thoracic imaging, additional channels must be available for parallel imaging techniques that are used in modern protocols.<sup>143,148</sup> More recently, receiver coils with up to 32 elements have been introduced.<sup>144</sup>

### Pulse Sequences

The standard pulse sequence for contrast-enhanced MRA is a spoiled three-dimensional (3D) T1-weighted gradient-echo sequence. It provides rapid imaging with acceptable resolution

and coverage, enabling the images to be acquired during breath holds. The 3D acquisition provides high spatial resolution across the imaged plane with no breaks between the individual partitions.<sup>138,141,142</sup> A “spoiled” sequence is one in which all residual transverse magnetization is destroyed before the next excitation. This increases the T1 weighting of the sequence and increases the contrast between the blood vessels and surrounding tissue.<sup>140</sup>

The repetition time of the MRA sequence should be as short as possible, as this setting will directly affect the acquisition time (TA) of the sequence:

$$TA = N_y \times N_z \times TR \quad (6.1)$$

where  $N_y$  is the number of phase-encoding steps in the  $y$  direction,  $N_z$  is the number of phase-encoding steps in the  $z$  direction (number of partitions), and TR is the repetition time. The TR should be shorter than 5 ms to maintain a reasonable duration of breath holding. High-performance scanners can now achieve TR times of less than 2 ms. This makes it possible to expand anatomical coverage without lengthening the acquisition time or losing spatial resolution, or to improve spatial resolution while maintaining the same degree of coverage. When a very short TR is used, a 3D dataset can be acquired multiple times in succession, resulting in a time-resolved MRA study.<sup>145,149</sup>

Analogously to the TR, the echo time TE should be as short as possible in MRA to minimize artifacts due to flow dephasing (e.g., in high-grade stenoses) and susceptibility differences (air–tissue interface in pulmonary angiography). Usually the TE is less than 2 ms, and high-performance scanners can achieve values less than 1 ms<sup>145,146</sup> (Fig. 6.42).

Various other techniques can be used to expedite data acquisition.<sup>139,142,148</sup> The use of partial Fourier techniques is based on the fact that information contained in the upper half of the raw data matrix duplicates information in the lower half. This makes it possible to carry out a complete image reconstruction with equivalent contrast and resolution using only slightly more than 50% of the raw data, enabling us to modify equation (6.1) as follows:

$$TA = N_y \times N_z \times TR \times 0.6 \quad (6.2)$$

The cost of this shortcut is reflected in the signal-to-noise ratio, which is decreased by the square root of the time saved (Fig. 6.42a).

As an alternative, slightly more than half of the raw data matrix can be scanned in the frequency-encoding direction. This registers only a portion of the complete signal echo. Also known as “fractional echo” or “asymmetric echo,” this technique allows a primary reduction of TE, leading secondarily to a shortening of TR.

Zero filling is an interpolation algorithm for improving the apparent resolution of individual images. With a zero filling factor of 2, the raw data matrix is doubled, the new points at the periphery of the matrix are filled with zeroes, and the images are then subjected to Fourier transformation. The use of zero filling does not primarily affect image acquisition, but it prolongs the reconstruction time. When zero filling is done in all three spatial planes with a filling factor of 2, eight times as

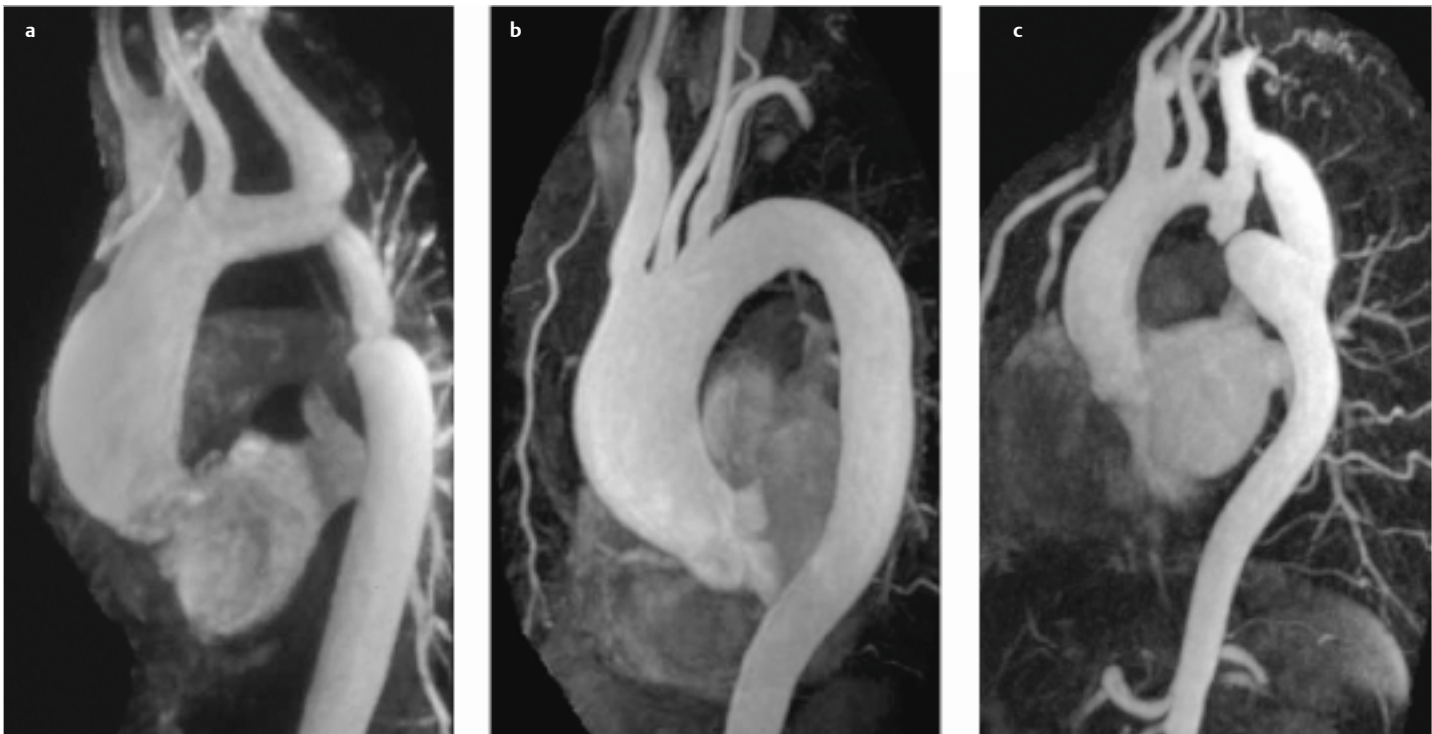


**Fig. 6.42a–c** Images showing the evolution of contrast-enhanced MRA in terms of scanner hardware and software. Note the progressive shortening of acquisition times and optimization of injection parameters.

**a** A total of 20 mL Gd-DTPA was injected at a rate of 2 mL/s, with an acquisition time of 28 s. The voxel size is 0.9 mm × 1.8 mm × 1.5 mm using partial Fourier techniques. A Dacron graft was placed in the proximal descending aorta for coarctation repair in this 65-year-old man.

**b** A high-performance gradient system and the use of parallel imaging resulted in an acquisition time of 11 s with a total contrast dose of only 15 mL injected at a rate of 4 mL/s. Voxel size is 1.0 mm × 1.0 mm × 1.2 mm. The patient was a 56-year-old man with ectasia of the ascending aorta.

**c** Time-resolved MRA with temporal resolution of 3.5 s and a total contrast dose of 10 mL injected at a rate of 4 mL/s. Voxel size is 1.3 mm × 1.3 mm × 1.5 mm. This 58-year-old woman underwent a subclavian artery-descending aorta bypass for coarctation of the aorta.

many voxels must be calculated as when interpolation is omitted. But if we assume that an imaging protocol provides sufficient diagnostic information without zero filling, we can use the zero filling strategy to reduce the number of necessary phase-encoding steps ( $N_y$  or  $N_z$ ), which in turn will shorten the acquisition time.

A recent approach to accelerated data acquisition is parallel imaging. In this technique the sensitivity profile of the coil elements used for signal detection is utilized for spatial encoding, so that ultimately the number of phase-encoding steps can be reduced at either the raw-data or image-data level.<sup>148</sup> Prior to application, the sensitivity profile of the coil elements that can be integrated into the imaging sequence must be determined by calibration. An acceleration factor of 2 leads to an ~48% reduction of acquisition time. The cost of this accelerated acquisition is reflected in the signal-to-noise ratio, which is decreased by a factor of  $1/\sqrt{\text{acceleration factor}}$  (Fig. 6.42b, c).



#### Essential Point

The current standard magnetic field strength for contrast-enhanced MRA of the thoracic vessels is 1.5T. The speed of data acquisition depends critically on the performance of the gradient system. The goal is to shorten the TR and TE times as much as possible. Partial Fourier techniques, zero filling, and parallel imaging have become established techniques for accelerating data acquisition. Parallel imaging requires multiple coil elements for signal detection and a corresponding number of interconnectable receiver channels

## Techniques of Examination and Interpretation

### Contrast Agents

The extracellular contrast agents that have been approved for clinical use are low-molecular hydrophilic gadolinium chelates. The agents that have been approved in Germany for MR angiography of the thoracic vessels are the open-chain complex Gd-DTPA (Magnevist, Bayer Schering Pharma), gadodiamide (Omniscan, GE Amersham Buchler), and the neutral macrocyclic agent gadobutrol (Gadovist, Bayer Schering Pharma). Gadobutrol is characterized by its double concentration of gadolinium compared with other extracellular contrast agents (1.0 mmol/L), so that only half as much needs to be injected to achieve an equal dose.<sup>146</sup>

The use of extracellular contrast agents temporarily shortens the T1 relaxation time of the blood to values between 30 and 80 ms.<sup>140,141</sup>

Original dose recommendations for MRA of the thoracic vessels were in the range 0.2–0.3 mmol/kg bw or a total dose of 40–60 mL. But with current acquisition times of 15–25 s it is sufficient to administer smaller doses in the range 0.1–0.15 mmol/kg bw, or a total dose of 20 mL.<sup>138,150,151</sup>

Considerable interest has focused on the development of “blood-pool” contrast agents that remain within the blood vessels for an extended period and cause little or no enhancement of extravascular tissues. In MRA of the great vessels, these blood-pool agents could make it possible to examine various regions without the need for additional contrast injection. They

would be particularly useful in the quantification of cardiac perfusion and imaging of the coronary arteries (see p. 111 ff)

### Bolus Timing

For successful contrast-enhanced MRA of the thoracic vessels, acquisition of the 3D dataset should coincide with the arrival of the contrast bolus in the vessels of interest.<sup>140,141,150</sup>

Various methods have been described for the optimum timing of contrast-enhanced MRA. In the test bolus method, a small initial bolus is administered to determine the physiological transit time of the contrast agent from injection to its appearance in the ROI so that MR data acquisition can be initiated precisely when the contrast bolus arrives in the target region (**Figs. 6.41, 6.42**).<sup>152</sup> There are also techniques in which continuous SI measurements are taken to time the arrival of the contrast bolus in a predefined test region. When the rise in SI per unit time exceeds a designated threshold, MRA is automatically initiated (e.g., Smart Prep, SmartScan). Another approach is the MR fluoroscopic detection of arrival of the contrast bolus in the target region with manual initiation of the MRA sequence (e.g., CareBolus).

Both methods involve centric rather than linear k-space acquisition, because ideally MRA is initiated to coincide with the peak concentration of gadolinium in the desired vessel. Large clinical studies have confirmed the reliability of these techniques in ensuring diagnostic image quality.<sup>146,150,153</sup> A major advantage of the test bolus method is that it can be used in any MR system and does not require special hardware or software.

The imprecise timing of contrast-enhanced MRA can affect image quality in various ways.<sup>154</sup> If the contrast bolus appears too early in the ROI relative to acquisition of the 3D dataset, the contrast agent will already have washed out by the time imaging is initiated, resulting in the undesired enhancement of veins and/or other vascular and tissue structures.

If the contrast bolus arrives too late, little or no contrast agent will be present in the vascular region of interest. “High-pass filter” artifacts may be observed; these occur when the T1 time of the blood changes rapidly because of contrast wash-in during acquisition of the central k-space lines, which determine image contrast. This results in poor visualization and enhancement of the target vessels, with or without “ringing” artifacts along the vessel walls, making it difficult to detect abnormalities.



#### Essential Point

For successful contrast-enhanced MRA of the thoracic vessels, acquisition of the 3D dataset should coincide with the arrival of the contrast bolus in the vessels of interest. Strategies for bolus timing include the test bolus method as well as manufacturer-specific automated or semiautomated techniques. The main advantage of the test bolus method is that it does not require special hardware or software.

### Planning the Examination

The pulmonary circulation can be imaged in one coronal or two sagittal slice packages<sup>151,155</sup>. In the coronal acquisition, both

halves of the lung are imaged simultaneously. Generally, a larger field of view is needed to prevent wrap-around artifacts from the shoulders and apposed arms, and this adversely affects the voxel size of the 3D dataset. Another option is to extend the arms above the head before imaging. The coronal technique is satisfactory for evaluating abnormalities of the pulmonary veins, but a 3D volume 12–14 cm thick cannot cover the entire pulmonary tree, and the voxel size remains anisotropic even when a high-end system is used. These restrictions may be overcome by use of multichannel phased-array coils, parallel imaging techniques, and imaging at 3T: here, whole coverage of the lung is realizable with acquisition of isotropic voxel sizes of 1 mm × 1 mm × 1 mm in a total of 20s.<sup>144</sup>

Sagittal data acquisition permits the use of smaller FOVs, which has a favorable effect on voxel size and makes it easier to acquire isotropic voxels. Because of the smaller 3D volume, the acquisition time is shorter than with coronal data acquisition. The main disadvantage of sagittal acquisition is the fact that separate datasets must be acquired for each side, which doubles the required contrast dose<sup>151,155–157</sup> (**Fig. 6.43**).

An oblique sagittal plane is usually recommended for imaging the thoracic aorta. Generally the prescription of this plane is based on the orientation of the aortic arch in the transverse plane. Coronal data acquisition is recommended in cases where it is necessary to investigate the supra-aortic branch vessels or detect congenital anomalies of the aortic arch.<sup>158–160</sup> ECG triggering is not absolutely essential but does improve visualization of the ascending aorta and is therefore recommended in examinations for ascending aortic disease.<sup>150</sup>

In time-resolved contrast-enhanced MRA, the time needed to acquire a 3D dataset can be shortened to less than 4s, which is a particular advantage in severely dyspneic patients. With the advent of multichannel coil technology, receiver channels and modified strategies for k-space sampling, the reduction of in-plane resolution, using thicker partitions, and decrease of the number of partitions may be minimized.<sup>139,143,145,161</sup> With time-resolved examination techniques, higher injection rates (up to 6 mL/s) should be used with a concomitant reduction in the contrast dose<sup>149</sup> (**Fig. 6.44**). Time-resolved imaging techniques can be useful in congenital vascular malformations (e.g., ductus arteriosus) and aortic dissections (perfusion characteristics of the true and false lumina), and to document steal effects in patients with subclavian artery stenosis.<sup>145,149,162</sup>

The recommended protocol for contrast-enhanced 3D MRA of the thoracic vessels is outlined in **Table 6.8**.



#### Essential Point

With acquisition times from 10 to 20 s, a contrast dose of 20 mL or 0.1–0.15 mmol/kg bw is generally adequate. The shorter the acquisition time, the higher the recommended injection rate (up to 4 mL/s). A rate up to 6 mL/s is recommended for time-resolved MRA.

### Interpretation

The interpretation of thoracic MRA is based on a detailed analysis of the source images. Combined with multiplanar refor-

# 7

## Heart Defects and Endocarditis

T. Buck, B. Plicht, T. Schlosser, and R. Erbel

### Congenital Heart Disease in Adults

Congenital cardiovascular anomalies are present in 0.8–1% of all newborns. The number of different anomalies is so large that their complete description would be beyond the scope of this book. This chapter therefore focuses on the capabilities of modern cardiac imaging techniques in the most common types of congenital heart disease in adults—atrial septal defects, patent foramen ovale, and ventricular septal defects.

#### ■ Atrial Septal Defect

##### Anatomy and Pathophysiology

Atrial septal defects (ASDs) account for ~10% of all congenital heart diseases and for 22–40% of congenital heart disease in adults. They are associated with varying degrees of left-to-right shunting of arterialized blood into the pulmonary circulation, depending on the size of the septal defect and the relative pressures. In extreme cases the shunt flow may be several times the volume flow of that in the systemic circulation. Atrial septal defects are primarily characterized by a volume overload on the right heart, which eventually lead to cardiac failure. With a left-to-right shunt above the level of the tricuspid valve, the great dilatatory capacity of the pulmonary vessels can forestall a pressure rise in the pulmonary artery and right ventricle. Comparable to the ventricular septal defect however, a functional and/or organic rise in vascular resistance will develop over time in the pulmonary circulation, causing the pressure in the right ventricle to rise. When the pulmonary vascular resistance exceeds that of the systemic circulation in the presence of a ventricular or atrial septal defect, a “shunt reversal” occurs, leading to marked cyanosis. This phenomenon is termed the **Eisenmenger reaction**.

Three etiological types of atrial septal defect are distinguished:

- An **ostium secundum atrial septal defect (ASD II)** is located in the central portion of the atrial septum in the region of the fossa ovalis. It is the most common type, accounting for 60–70% of atrial septal defects.
- An **ostium primum atrial septal defect (ASD I)** is usually a large defect that comprises 15–25% of atrial septal defects. It results from a failure of fusion of the septum primum with the endocardial cushion between the atrioventricular valves. As a result, it is commonly associated with mitral valve defects and occasionally with tricuspid valve defects.
- A **sinus venosus atrial septal defect** is present in 5–15% of cases. It occurs in the posterosuperior portion of the atrial septum between the termination of the superior vena cava

and the fossa ovalis. It is frequently associated with anomalous termination of the right pulmonary veins in the right atrium.

##### Clinical Features

###### Symptoms

- Generally asymptomatic until the third decade; 70% of patients are symptomatic by the fifth decade
- Dyspnea, rapid fatigability (manifestations of heart failure).
- Palpitations (in patients with atrial arrhythmias)
- Proneness to respiratory infections
- Approximately 15% of patients show clinical symptoms of associated mitral insufficiency

###### Complications

- Atrial fibrillation or flutter
- Mitral insufficiency

##### Imaging

###### Echocardiography

###### 2D Echocardiography

- Transthoracic scanning enables direct visualization of the septal defect (excepting sinus venosus defects) (**Fig. 7.1**).
- Transesophageal scanning permits direct visualization of a sinus venosus defect (**Fig. 7.2**).
- Enlargement of the right atrium and right ventricle
- Detection of associated congenital anomalies

###### 3D Echocardiography

- Enables direct visualization of the ASD in the frontal view to assess the location, size, and shape of the defect.
- Can detect an AV canal in patients with ASD I.
- Allows direct visualization of a cleft in the anterior mitral valve leaflet in ASD I.

###### Color Doppler Echocardiography

- Detection of shunt flow by demonstrating a flow jet through the atrial septum into the right atrium
- Frequently primary detection of a sinus venosus defect is based on an abnormal flow signal near the termination of the superior vena cava (**Fig. 7.2b**).
- Detection of an AV canal in patients with ASD I
- Detection of associated mitral insufficiency in ASD I

###### Contrast Echocardiography

- Detection of a left-to-right shunt based on the washout phenomenon in the contrast-filled right atrium (**Fig. 7.1b**).

**CW Doppler Echocardiography**

- Pulmonary hypertension can be diagnosed by assessing the systolic pulmonary artery pressure based on the regurgitant signal from the tricuspid valve.

**Essential Point**

In the presence of clinical suspicion of a left-to-right shunt at the atrial level, it is possible to overlook a high-sited sinus venosus type of ASD if the atrial septum appears normal. Often a sinus venosus defect can be detected only by multiplanar transesophageal echocardiography in color Doppler mode.

**Magnetic Resonance Imaging and Computed Tomography**

The standard planes for detecting an ASD in MRI are horizontal long-axis slices and short-axis slices through the heart. Spoiled gradient-echo sequences are preferred. They are of advantage over SE and balanced SSFP sequences in that they can also detect smaller defects by the associated zones of turbulent flow, for example.

Determination of the maximum size of the ASD is essential in selecting patients for interventional repairs, an unsuitable procedure for large defects. Both MRI and multislice CT (MSCT) can document the enlargement of the right atrium and right ventricle (**Fig. 7.3a**). In addition to demonstrating morphologi-

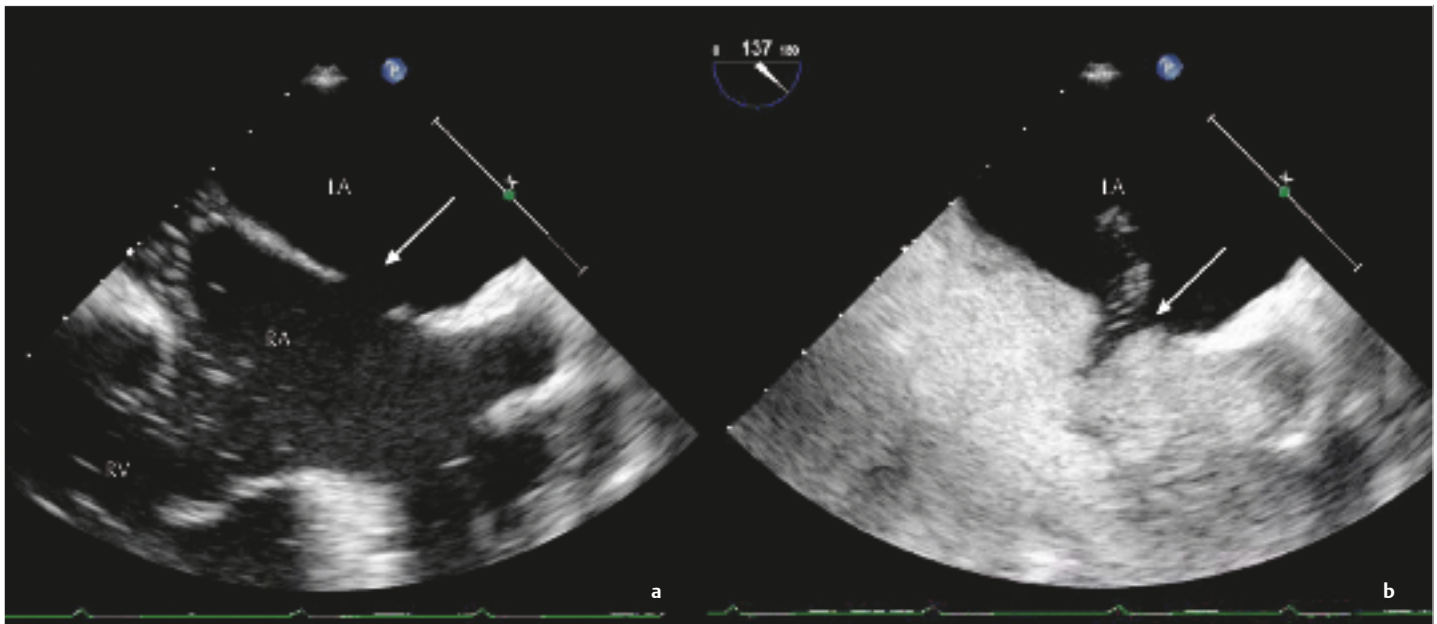


**Fig. 7.1 a, b** Transesophageal echocardiography of ASD II (arrow).  
a Prior to contrast wash-in.

b Typical appearance of the washout phenomenon (arrow) in a left-to-right shunt at the atrial level. Various bubbles can be seen entering the left atrium after passing through the shunt.

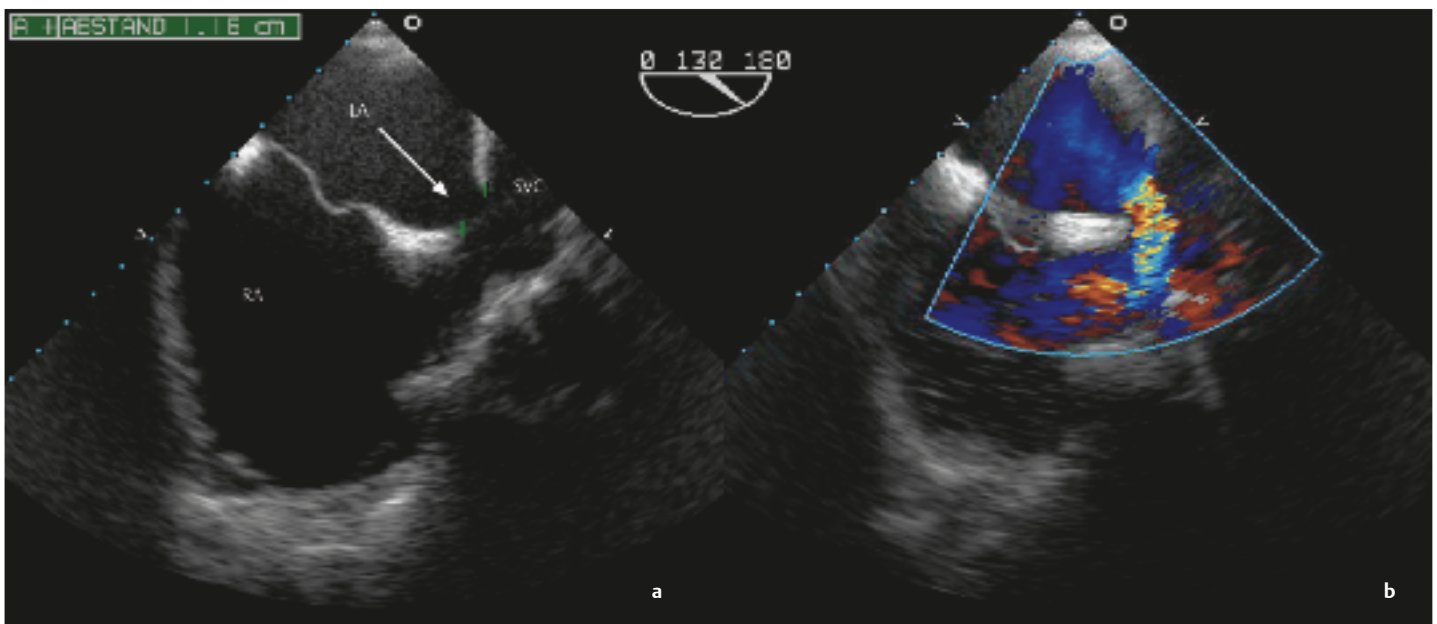


**Fig. 7.2 a, b** Sinus venosus atrial septal defect documented by transesophageal echocardiography.

a The size of the defect (arrow) is measured at the entry of the superior vena cava into the right atrium.  
b Abnormal flow signal detected by color Doppler echocardiography.



cal features, MRI also enables an accurate assessment of the  $Q_p/Q_s$  ratio based on flow measurements in the ascending aorta and pulmonary trunk. This ratio is important in selecting patients for operative or interventional repair.<sup>1</sup> The  $Q_p/Q_s$  ratio can also be determined using cine MRI to identify right and left ventricular stroke volumes, provided the presence of an additional significant valvular defect can be excluded. MRI and CT additionally detect any anomalous pulmonary venous termination that may be present. Operative treatment is the only option available for correcting this anomaly<sup>2</sup> (Fig. 7.3b).

## ■ Patent Foramen Ovale

### Anatomy and Pathophysiology

Patent foramen ovale (PFO) is a valvelike opening that persists postnatally between the septum primum and secundum in the region of the fossa ovalis owing to failed fusion of these septal elements. A right-to-left shunt at the atrial level may occur spontaneously or in response to a Valsalva maneuver. Autopsy results indicate that PFO has a prevalence of ~25% in the general population. Its clinical significance is that it places patients at risk for paradoxical emboli. This risk appears to be particularly high in patients with a hypermobile atrial septal aneurysm, which frequently coexists with PFO. Because the opening and volume of the shunt are generally small, hemodynamic complications do not occur.

### Clinical Features

#### Symptoms

- The majority of patients with PFO are asymptomatic.

#### Complications

- Central or peripheral emboli, stroke, transient ischemic attacks, dizzy spells, migraines

### Imaging

#### Echocardiography

##### M-Mode Echocardiography

- M-mode can document hypermobile excursions associated with an atrial septal aneurysm (Fig. 7.4a).

##### 2D Echocardiography

- Demonstrates the valvelike separation between the septum primum and secundum; but cannot reliably detect patent foramen ovale (2D visualization only by transesophageal scanning).
- Can detect an atrial septal aneurysm (frequently also detectable by transthoracic scanning).

##### Contrast Echocardiography

- Can reliably detect or exclude patent foramen ovale based on the right-to-left passage of contrast medium, either spontaneously or in response to a Valsalva maneuver (Fig. 7.4b).

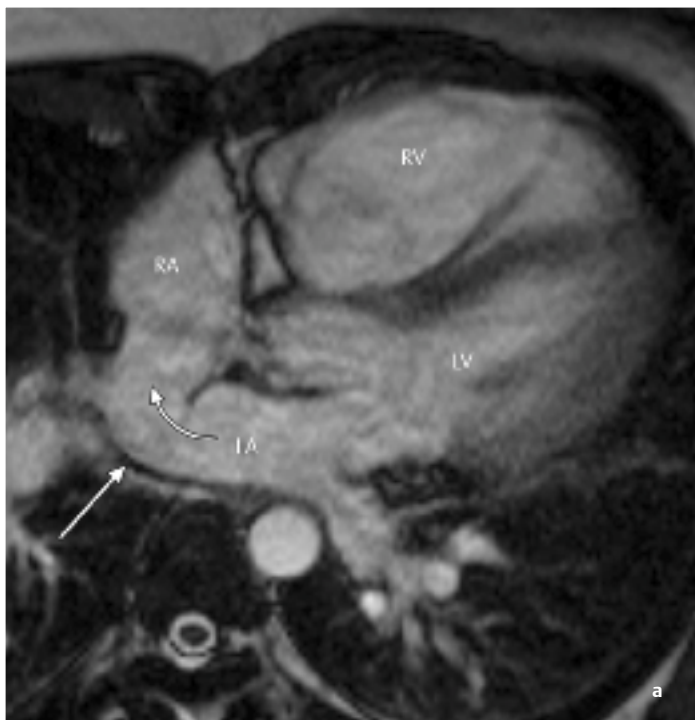


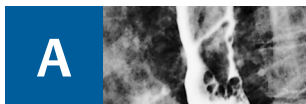
**Fig. 7.3 a, b** Large ASD II in a 32-year-old woman.  
**a** Cine image in the four-chamber view demonstrates the large ASD (arrow).

**b** Contrast-enhanced 3D MRA further demonstrates partial anomalous pulmonary venous termination on the right side. The upper and middle lobe veins (arrows) open into the superior vena cava.

# Index

To view the use of specific modalities in specific clinical conditions, the reader is advised to locate and read the specific conditions. This is because all but the least common imaging or most specialized imaging modalities and techniques are mentioned repeatedly under each clinical condition in the section on "heart disease." References to the modalities in that section, generally, have *not* been included in the index (with certain exceptions where they have *also* been mentioned in the "modalities" section). Under main entries for individual modalities, the reader

will *only* find page references from the "modalities section" (detailing general principles and applications). Under the main entries for specific diseases and conditions the reader will find references to specific modalities, *only* if they have been mentioned in the "modalities" section. Figures and tables are comprehensively referred to from the text. Therefore, significant material in figures and tables has only been given a page reference in the absence of their concomitant mention in the text referring to that figure. "vs" indicates the differential diagnosis of conditions.



**A**

A-mode ultrasound 35

abdominal aorta

- angiography (aortography) 61
- balloon fenestration, intravascular ultrasound 65

acipimox in FDG-PET 72

acoustic quantification 35

- chronic CAD 190

acute aortic syndrome 271-80

acute coronary syndrome, pathogenesis 172-3

adenosine, perfusion MRI 113

- in chronic CAD 190

Agatston calcium score 76, 77, 178, 181

ammonia, <sup>15</sup>N-labelled, for PET 72

amyloidosis 222

Anderson-Fabry disease 224

anesthesia, cardiac catheterization 59

aneurysm

- aortic 267-71
  - imaging 29-30, 86-7, 268-71
- cardiac 22, 198-200, 234, 242
  - radiography 22
  - ventricular 198-200
- coronary, in Kawasaki disease 127
- pulmonary artery 262

angina pectoris 3, 188

- angiography 63, 64
- in aortic stenosis 156
- in mitral stenosis 147
- stable 188
- vasospastic 201

angiocardiology, conventional 59-61

- complications 62
- indications/contraindications 62
- selective 61-2

angiography 59-67

- conventional 59-67
- coronary *see* computed tomographic angiography
- MR *see* magnetic resonance angiography

angioplasty, percutaneous transluminal

- coronary *see* percutaneous balloon transluminal angioplasty

angiosarcoma 234, 238-9

angiосcopy, atherosclerosis and atherosclerotic plaque 173, 176

aorta (thoracic and in general)

- angiography (aortography)
  - conventional 61
  - CT 86-7
  - MR 131-2
- disorders and abnormalities 264-82
  - acquired 265-80

*see also specific abnormalities e.g.*

- aneurysm; coarctation; dissection; sclerosis;
- traumatic aortic injury
  - congenital 28, 88, 264-5

echocardiographic determination, diameter 42

FDG-PET of inflammatory changes 74

intravascular ultrasound, diagnostic and therapeutic use 65

radiography 28-30

aorta angusta 29

aortic sinus (sinus of Valsalva), aneurysm 242

aortic valve 155-61

- bicuspid 161, 267, 272, 275
- in hypertrophic cardiomyopathy 219
- insufficiency/regurgitation 158-61
  - in aortic dissection 275
  - clinical features 159
  - etiology 158
  - imaging 48, 50, 110, 159-61
  - mitral insufficiency combined with 162
  - mitral stenosis combined with 162
  - pathophysiology 158-9
- MRI of normal valve 97
- stenosis 155-8
  - clinical features 156
  - etiology 155
  - imaging 110, 156-8
  - mitral insufficiency combined with 162
  - mitral stenosis combined with 162
  - pathophysiology 155

aortitis 280

aortocoronary bypass grafts 201, 205

apical ballooning syndrome 227

aplasia, pericardial 250-1

arrhythmias 3-4

arrhythmogenic RV dysplasia/cardiomyopathy 23, 215, 225-7

- epidemiology/pathophysiology/clinical features 225-6
- imaging 226-7
- radiography 23

arterial grafts for coronary bypass 201, 203

arterial sclerosis *see* atherosclerosis

arteriovenous malformations, pulmonary 260

MR angiography 132-3

ascending aorta

- anatomy 264
- angiography 61

asymmetric echo, MR angiography of great vessels 128

atheroma 171, 172

atherosclerosis/arterial sclerosis

- aortic 28, 29, 265-7, 277, 278-9
- coronary 171-81
  - imaging 116, 174-81, 174
  - pathogenesis 171-3
  - plaque *see* plaque
  - subclinical signs 171-81

atrioventricular connections, concordant vs discordant, MRI 102-3

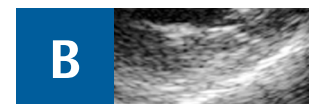
atrium/atria

- enlargement
  - both, in restrictive cardiomyopathy 221
  - LA, radiograph 9-10
  - RA, radiograph 8
- fibrillation, catheter ablation 261
- lymphoma, LA 239
- septum
  - aneurysm 242
  - defect 141-3
  - fatty infiltration/lipomatous hypertrophy 234, 236
- situs 102
- volume, LA, echocardiographic estimation 43

attenuation correction (myocardial scintigraphy) 68

autoregulation, coronary vessels 65-6

axial cine-steady-state free precession 96



**B**

B-mode ultrasound 25

bacterial endocarditis *see* endocarditis

balloon dilatation, percutaneous *see* percutaneous balloon transluminal angioplasty

balloon fenestration of abdominal aorta, intravascular ultrasound 65

Behçet disease 252

bicuspid aortic valve 161, 267, 272, 275

bioprosthetic valves 166, 168

biopsy, endomyocardial *see* endomyocardial biopsy

biventricular pacing in dilated cardiomyopathy, echocardiographic criteria 216-17

blood flow/pressure *see* flow; pressure

bolus timing, contrast-enhanced MRA of great vessels 130

brachial artery approach to coronary angiography 63

breathing in MR coronary angiography

- breath-hold 121, 123-4
- free 124

breathlessness (dyspnea) 3

bright-blood sequences (MRI) 92

- morphological imaging 98

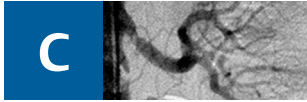
"bright is dead" rule 196

broadband scattering 34

bronchial artery position in atrial situs 102

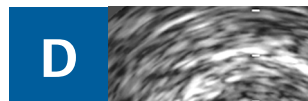
bronchial carcinoma invading pulmonary arteries 261-2

bypass grafts in CAD 201-8



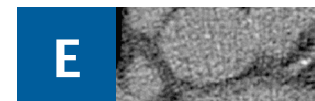
C-reactive protein test 180  
 calcifications  
   cardiac, radiography 5, 6  
   coronary 171  
     intravascular ultrasound 65  
     stented vessel 209  
 calcium, coronary 171  
   determination 76-8, 81  
 cancer *see* malignant tumors  
 capillary hemangioma, pulmonary 259-60  
 carcinoma, bronchial, invading pulmonary arteries 261-2  
 cardiac disease and function *see* heart disease and specific functional parameters *e.g.*  
   ejection fraction; output; rate  
 cardiomyocytes in chronic CAD 188  
 cardiomyopathies 215-27  
   dilated *see* dilated cardiomyopathy  
   hypertrophic *see* hypertrophic cardiomyopathy  
   infiltrative 222-4  
   radiography 22-3  
   restrictive *see* restrictive cardiomyopathies  
   unclassified and secondary 23, 215, 216, 227  
 catheter ablation, atrial fibrillation 261  
 catheterization  
   for angiocardiology 59-62  
   for intravascular ultrasound 64  
 chambers, cardiac  
   enlargement *see* enlargement  
   radiographs 5-10  
 chest pain  
   aortic syndrome (incl. dissection) 271, 272  
   differential diagnosis 3  
   ischemic/cardiac *see* angina pectoris  
 Chiari network 242  
 chordae tendinae rupture 150  
 cine sequences, ventricular aneurysm 199  
 cine steady-state free precession (SSFP)  
   sequence 100  
   axial 96  
 clinical manifestations of heart disease 3-4  
 coarctation, aortic 28-9, 265  
   MR angiography 131-2  
 coherent motion in tissue Doppler echocardiography 45  
 collateral vessels in myocardial ischemia and infarction 181-3  
 collimation, CT coronary angiography 81  
 color Doppler 45  
   transmitral inflow 47  
 color kinesis 35  
   chronic CAD 190, 195  
 computed tomographic angiography  
   coronary vessels 80-4  
   great vessels 84-8  
   renal failure contraindicating 254  
 computed tomography 76-90  
   multislice *see* multislice spiral CT  
   pericardial 243  
   principles 80  
   *see also* positron emission tomography/CT  
 concordant motion in tissue Doppler echocardiography 46  
 congenital cardiovascular anomalies (and congenital heart disease) 101-2, 141-6  
   aorta 28, 88, 264-5  
   CT angiography  
     coronary vessels 84  
     great vessels 88  
   MR angiography  
     coronary vessels 126  
     great vessels 131-3  
   MRI 101-2  
   pulmonary vessels 260-1

radiography, great vessels (incl. aorta) 28  
 tumors vs 242  
 congestion, pulmonary 12, 18, 21  
 consent, informed  
   cardiac catheterization 59  
   CT coronary angiography 80  
 constrictive pericarditis 27, 247-50  
   anatomy/pathophysiology/clinical features 247  
   hypertrophic cardiomyopathy vs 221  
 continuity equation 50  
 continuous-wave Doppler 44  
 contractility (myocardial)  
   in ischemia 180-1  
   LV, echocardiographic assessment 52  
 contrast echocardiography 37  
 contrast mechanisms in MRI  
   in coronary MR angiography 124-5  
   with pathological 98  
 contrast media/agent  
   conventional angiography, test injection 60  
   CT angiography of coronary vessels 81  
     adverse events 80  
   CT angiography of great vessels 84, 85  
   echocardiography 37  
   MR angiography  
     coronary vessels 125-6  
     great vessels 129-30  
   MRI 113  
     administration in delayed-enhancement imaging 120  
 contrast radiography, esophagus 5  
 cor pulmonale 15-16, 25  
 coronary angiography  
   conventional 63-4  
   CT 80-4  
   MR 121-7  
 coronary angioplasty *see* percutaneous balloon transluminal angioplasty  
 coronary artery  
   aneurysms in Kawasaki disease 127  
   angiography *see* coronary angiography  
   anomalies *see* congenital cardiovascular anomalies  
   atherosclerosis *see* atherosclerosis  
   calcium *see* calcifications; calcium plaque *see* plaque  
   stenosis *see* stenosis  
 coronary artery disease (CAD; coronary heart disease; CHD) 22-3, 171-214  
 chronic (incl. chronic myocardial ischemia and late sequelae of MI) 187-201  
   cardiomyopathy in 217  
   clinical features 188  
   diagnosis 188-200  
   pathophysiology 187  
 early detection 171  
 imaging 171-214  
   CT angiography 83-4  
   Doppler intravascular ultrasound 65-6  
   intravascular ultrasound 65, 174, 193  
   myocardial scintigraphy 70-1  
   postoperative and postinterventional 201-10  
   radiography 22-3  
   prevention 176-81  
   *see also* acute coronary syndrome  
 coronary stent 201, 208-10  
 crista terminalis 242  
 cross-sectional area of valve orifice 50  
 cyanosis 3  
 cysts, pericardial 244-5



Dallas criteria 227  
 dark-blood sequences (MRI) 92

morphological imaging 98, 99  
 DeBakey classification of aortic dissection 30, 271, 272  
 degenerative disorders/change  
   aorta 265-71  
   aortic valve 155, 158  
   mitral valve 150, 154  
 delay time, myocardial return to start position in MRI 99, 100  
 delayed-enhancement MRI *see* late enhancement MRI  
 descending (thoracic) aorta  
   anatomy 264  
   dissection (=type B) 271, 272, 273, 274-5  
   right 28, 264  
 dextrocardia, mirror-image 17  
 dextroposition 17  
 dextroversion 17  
 diabetes, myocardial scintigraphy 71  
 diameter  
   cardiac *see* size  
   coronary stent 209  
 diastole  
   echocardiographic studies in  
     pulmonary arterial pressure 51  
     ventricular function/dysfunction 54-5  
   in restrictive cardiomyopathy, severe dysfunction during 221  
 dilatation *see* enlargement  
 dilated cardiomyopathy 23, 24, 215, 215-18  
   epidemiology/pathophysiology/clinical features 215-16  
   imaging 216-18  
     radiography 23, 24  
 dipyridamole, perfusion MRI 113  
 in chronic CAD 193  
 dissection, aortic 30, 271  
   CT angiography 86-7  
   intravascular ultrasound 30  
   radiography 30  
   traumatic *see* traumatic aortic injury  
 diverticula, pericardial 244-5  
 dobutamine stress  
   in chronic CAD 188-9, 191, 194, 195-6  
   echocardiography 38  
   MRI 107  
   perfusion studies 113  
 Doppler ultrasound  
   heart (Doppler echocardiography) 44-7  
   hemodynamic assessment 48, 49, 50  
   reference values 46  
   systolic LV function 52  
   intracoronary 65-6  
   tissue *see* tissue Doppler  
 double aortic arch 28, 264  
 double-disk valves 166, 168, 169  
 double-oblique sections of the heart (MRI) 92  
 dual-source CT 80  
 DuBois formula 104  
 dyskinesia, ventricular aneurysm 198, 199  
 dyspnea 3  
 dysrhythmias 3-4



ECG *see* electrocardiography  
 echocardiography 34-58  
   basic principles 34-6  
   examination techniques 40-2  
   pericardial 243  
   quantification using 41-3  
   specific applications 37-40  
 Echovist-300 37  
 edema 3  
   myocardial (ischemic-reperfused myocardium) 184  
   pulmonary, in chronic heart failure 18

effusions  
 pericardial 25, 26, 27, 245, 246  
 in aortic dissection 275  
 imaging 27, 243, 244, 246, 247  
 pleural *see* pleural effusions  
 ejection fraction, MRI determination 104  
 electrocardiography (ECG)  
 in CT angiography  
 coronary vessels 81  
 great vessels 86  
 in MRI 91  
 ECG-triggered sequences 105, 105-6  
 sarcoidosis 223  
 electrocardiography-gated myocardial scintigraphy 68-9  
 electron beam CT of coronary vessels 80, 180  
 calcium determination 76-8  
 elongation, aortic 29  
 emboli, pulmonary 21, 252-6  
 acute 252-5  
 clinical classification 252  
 clinical features 252  
 diagnosis 252  
 pathophysiology 252-3  
 risk factors 252  
 chronic recurrent 20, 21, 255-6  
 imaging 253-5  
 CT angiography 87-8, 253-4  
 radiography 20, 21  
*see also* microemboli; thromboembolic  
 pulmonary hypertension, chronic  
 endocardial tumors 232  
 endocarditis (infective/bacterial)  
 aortic valve 160  
 mitral valve 152  
 prosthetic valve dysfunction 166, 169  
 endocrine causes of hypertension 24  
 endomyocardial biopsy  
 cardiomyopathies 215  
 sarcoidosis 223  
 myocarditis 227  
 endomyocardial disease 224-5  
 enlargement/dilatation  
 aorta 29  
 chambers 5-10  
 atria *see* atrium  
 diseases leading to 11, 18, 20  
 radiographs 5-10, 11  
 enzyme replacement therapy in Anderson–  
 Fabry disease 224  
 esophagus  
 contrast radiography 5  
 echocardiography via 39, 40-1  
 EuroSCORE 181  
 exercise stress imaging  
 echocardiography 38  
 MRI 107  
 perfusion studies 113



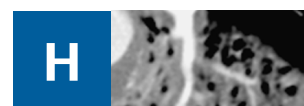
failure, heart 17-21  
 acute 17, 20  
 causes 13, 17  
 chronic 17-21  
 causes 12, 17  
 radiography 17-21  
 global 21  
 left 19  
 right 20  
 fast low-angle shot (FLASH) MRI 105, 106  
 fast spin-echo sequences *see* turbo spin-echo  
 sequences  
 fat suppression  
 MR coronary angiography 125  
 MRI 98

fatty infiltration (lipomatous hypertrophy) of  
 atrial septum 234, 236  
 fatty streaks 171, 172  
 FDG *see* fluorodeoxyglucose  
 females with coronary heart disease, myocar-  
 dial scintigraphy 71  
 femoral artery catheterization  
 coronary angiography 63  
 intracardiac angiography 59-60  
 fibrinous pericarditis 26, 245  
 fibroatheroma 171  
 fibroelastoma 233, 236  
 fibroma 233, 238  
 fibrosis  
 endomyocardial 225  
 pericardial, in constrictive pericarditis  
 247  
 Fick method, cardiac output measurement  
 60, 61  
 filling pressures, LV, echocardiographic studies  
 50, 55-6  
 first-pass perfusion MRI 112  
 FLASH MRI 105, 106  
 flow (blood)  
 in coronary bypass graft 206  
 Doppler echocardiography studies 44, 45  
 reference values for flow velocity 46, 47  
 Doppler studies in coronary vessels 65-6  
 MRI  
 flow compensation 105  
 measurement 108-9  
 regional myocardial flow as indicator of  
 perfusion 111  
 pulmonary, decreased 15  
 shunt, echocardiographic studies 49  
 fluorodeoxyglucose (FDG)-PET 71-2, 72  
 hibernating myocardium 73, 195  
 plaque imaging 73, 74  
 fluoroscopy, preliminary 5  
 foramen ovale, patent 143-4  
 four-chamber view (MRI) 94  
 Fourier techniques, MR angiography of great  
 vessels 128  
 fractional echo, MR angiography of great  
 vessels 128  
 fractional flow reserve (FFR), myocardial 66  
 Framingham Study 176, 181  
 free-breathing in MR coronary angiography  
 124  
 frequency-encoding direction, MR angiography  
 of great vessels 128  
 frontal radiograph *see* posteroanterior radio-  
 graph



gadolinium (paramagnetic)-enhanced MR  
 studies 113  
 late *see* late enhancement MRI  
 MR angiography  
 coronary 125-6  
 great vessels 129-30  
 gamma cameras for SPECT 68  
 gastroepiploic artery for coronary bypass 203  
 gated myocardial scintigraphy 68-9  
 gelatin solution in contrast echocardiog-  
 raphy 37  
 glucose metabolism, myocardial 72  
 gradient-echo (GE) sequences 92  
 coronary bypass 203  
 functional imaging 105, 106-7  
 great vessels 128  
 intracardiac thrombi 241  
 great vessels 252-63  
 CT angiography 84-8  
 MR angiography 127-33  
 guidewire

cardiac catheterization 59  
 intracoronary Doppler 65



heart disease (in general)  
 clinical manifestations 3-4  
 pulmonary vascular pressure changes due to  
 12  
*see also specific types of disease/disorders/  
 dysfunction e.g.* arrhythmias; coronary heart  
 disease; failure  
 heart function/physiology *see specific paramet-  
 ers e.g.* ejection fraction; output; rate  
 Heinz–Nixdorf Recall Study 180  
 helical CT *see* spiral CT  
 hemangioma  
 cardiac 233, 237  
 pulmonary vascular 259-60  
 hemochromatosis, cardiac 216  
 hemodynamics 48-51  
 coronary, Doppler studies 65, 66  
 echocardiographic assessment 48-51  
 pulmonary  
 pulmonary vascular changes due to  
 alterations in 13  
 radiography 11-12  
 in restrictive cardiomyopathies 221  
 hemorrhage or hematoma  
 aortic intramural 277  
 coronary plaque 172, 173  
 heterotaxy syndrome 102  
 histology, virtual, atherosclerotic plaque  
 175-6  
 history-taking, coronary CT angiography 80  
 horizontal long axis of LV (MRI) 94  
 Hounsfield units/scale 80  
 Hughes–Stovin syndrome 252  
 hyperemia, pulmonary 15  
 hypereosinophilic syndrome 225  
 hyperplasia of atrial septum, fatty 234  
 hypertension 3, 23-5  
 pulmonary arterial *see* pulmonary arterial  
 hypertension  
 systemic/arterial 4, 23-5  
 hypertrophic cardiomyopathy 23, 215, 218-21  
 epidemiology/pathophysiology/clinical  
 features 218  
 imaging 23, 218-21  
 obstructive 215, 218, 219  
 hypertrophy  
 atrial septum, lipomatous (=fatty deposits)  
 234, 236  
 ventricular 11  
 hypoplasia of aortic arch, congenital 264  
 hypotension, cardiac 4



incoherent motion in tissue Doppler echocar-  
 diography 45  
 indium-111-labelled monoclonal antibody,  
 myocarditis 229  
 inertial mass 50  
 infections  
 endocardial *see* endocarditis  
 myocardial 228, 229  
 inflammatory activity, reperfused myocardium  
 184  
 inflammatory aortic disease 280  
 inflow tract of ventricles, MRI  
 LV 95  
 positional anomalies 102

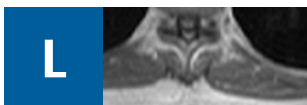
informed consent *see* consent  
 integrated scatter 34-5  
 interstitial pulmonary edema 18  
 intima  
   tear and flap in aortic dissection 272, 273, 274, 274-5, 275  
   thickening 171, 172  
     detection 65, 180  
 intracardiac echocardiography 39-40  
 intracardiac pressure evaluation  
   catheterization techniques 60  
   echocardiographic techniques 50-1  
   *see also* ventricles  
 intracardiac shunts *see* shunts  
 intraoperative echocardiography 39  
 intravascular ultrasound 64-6  
   CAD 65, 174, 193  
   myocardial bridging *see* myocardium  
 invasive imaging techniques 64-6  
   coronary artery disease, review of 174  
 inversion (and situs inversus), cardiac  
   MRI 101-2  
   radiography 17  
 inversion pulse (MRI)  
   delayed-enhancement imaging 117, 118  
   morphological studies 98, 99  
   perfusion studies 112  
 inversion-recovery sequences 117, 120  
   in coronary MR angiography 125-6  
   of intracardiac thrombi 241  
   phase-sensitivity 118  
 inversion time  
   delayed-enhancement imaging 118  
   perfusion MRI 112  
 iodine concentration of contrast medium in CT  
   coronary angiography 81  
 ischemia, myocardial *see* myocardial ischemia  
 ischemic cardiomyopathy 217



Judkins technique 63



Kawasaki disease, coronary MR angiography 127  
 Kerley A and B lines 19  
 kidney *see entries under* renal



late (delayed) enhancement MRI 116-21  
   hypertrophic cardiomyopathy 219-20  
   infiltrative cardiomyopathies  
     amyloidosis 222  
     sarcoidosis 223-4  
   myocardial hibernation 194-5  
   myocardial scar/chronic infarction 196  
   myocarditis 229-30  
 lateral radiograph 4-5  
   atrial enlargement, right  
     ventricular enlargement  
       left 8  
       right 6  
 leiomyosarcoma, pulmonary vascular 256-9  
 Levovist 37  
 lipoma 233, 234-6  
 lipomatous (fatty) infiltration of atrial septum 234, 236

liposarcoma 238  
 local anesthesia, cardiac catheterization 59  
 Löffler syndrome 225  
 lumen in aortic dissection  
   false 272, 274  
   true 274  
 Luminit 37  
 lungs  
   carcinoma invading pulmonary arteries 261-2  
   congestion 12, 18, 21  
   edema in chronic heart failure 18  
   perfusion mapping with CT 254  
 lymphangioma 233, 238  
 lymphatic system 16  
 lymphoma, primary 234, 239



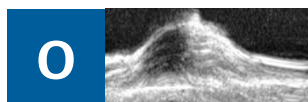
M-mode echocardiography 35  
   color Doppler 45  
   LV function 51  
   quantification using 41  
 magnetic resonance angiography 121-33  
   coronary arteries 121-7  
   great vessels 127-33  
 magnetic resonance imaging 91-137  
   clinical applications 110  
   function 104-10  
   gradient-echo *see* gradient-echo sequences  
   morphology 98-103  
   pericardial 243-4  
   planning the examination 91-7  
   spin-echo *see* spin-echo sequences  
 malignant tumors  
   cardiac 232, 238-40  
     MRI signal characteristics 234  
     pericardial 238-9, 239-40, 240, 250  
     secondary *see* metastases  
   pulmonary vascular 256-9, 261-2  
 malposition  
   MRI 101-2  
   radiography 17  
 mammary artery, internal, for coronary bypass 201, 203  
 mass (pathological lump)  
   neoplastic *see* tumors  
   nonneoplastic 240-2  
 mass (physical quantity)  
   calcium, determination 77-8  
   myocardial *see* myocardium  
 maximum intensity projection, contrast-enhanced MR angiography 130  
 mechanical heart valves 166, 167  
 medial thickening 180  
 mesothelioma, pericardial 234, 239-40  
 metabolism, ischemic myocardium 180-1  
 metaiodobenzylguanidine (MIBG) scintigraphy 73  
 metastases, cardiac 232, 234, 240  
   pericardium 240, 250  
 MIBG scintigraphy 73  
 microemboli, coronary 176  
 mirror-image dextrocardia 17  
 mitral valve 147-54  
   annulus velocity, Doppler studies 46-7  
   defects (in general) 147-54  
     radiography 9  
   flow velocity, Doppler studies 46, 47  
   in hypertrophic cardiomyopathy 219  
   insufficiency/regurgitation 150-4  
     aortic insufficiency combined with 162  
     aortic stenosis combined with 162  
     etiology 150  
     imaging 49, 50, 110, 152-4  
     pathophysiology 150-1  
   MRI of normal valve 96, 97

orifice area, echocardiography studies 49, 50  
 prolapse 150, 151  
 prosthetic 168, 169  
 stenosis 147-50  
   aortic insufficiency combined with 162  
   aortic valve insufficiency combined with 162  
   clinical features 147  
   echocardiographic studies 49, 50, 148-9  
   etiology 147  
   insufficiency accompanying 151  
   MRI 250  
   pathophysiology 147  
   radiography 9  
 motion  
   cardiac/ventricular wall  
     in acute ischemia 186  
     in arrhythmogenic right ventricular cardiomyopathy 226  
     artifacts due to, CT coronary angiography 82  
     in chronic ischemia 189, 198  
     compensation in MR coronary angiography for 122  
     echocardiographic studies 52-4  
     MRI studies 104-7, 186  
     with ventricular aneurysm 198  
   respiratory, compensation in MR coronary angiography for 123-4  
 multiplanar reformation 82  
 pulmonary embolism 254  
 multislice spiral (helical) CT  
   coronary vessels 80  
     bypass grafts 202-3  
     calcium determination 78-9  
     in chronic CAD 193, 200  
     stents 208, 209-10  
   great vessels 86  
 mural thrombosis 173  
 myocardial infarction 181  
   delayed-enhancement MRI, acute and chronic MI 120  
   infarct size and its determinants 181-3  
   late sequelae *see* coronary artery disease, chronic  
   radiography (acute and chronic) 22  
 myocardial ischemia 181-201  
   acute 181-6  
     pathophysiology 181-3  
   chronic *see* coronary artery disease, chronic  
   imaging 181-6  
     perfusion MRI 114, 186  
   reperfusion following *see* reperfusion  
   review of invasive and noninvasive tests 174  
 myocarditis 227-30  
   epidemiology/pathophysiology/clinical features 227-8  
   imaging 228-30  
 myocardium  
   bridging 201  
     intravascular ultrasound 65, 66, 201  
   contractility *see* contractility  
   edema (ischemic-reperfused myocardium) 184  
   fractional flow reserve (FFR<sub>myo</sub>) 66  
   hibernation 184, 187, 194-5, 200  
     imaging 73, 194-5, 195  
   mass determination 104  
     LV, echocardiographic estimation 41  
   metabolism in ischemia 180-1  
   metastases 240  
   motion *see* motion  
   perfusion *see* perfusion; reperfusion  
   primary disease *see* cardiomyopathies  
   scar 185, 188, 195-8, 200  
     imaging 73, 195-8, 198  
   scintigraphy *see* scintigraphy  
   strain 47  
   stunning 184, 194

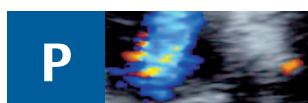
tagging 107-8  
 viability, assessment 71, 72, 73, 184, 198  
 wall *see* wall  
 myxoma 233-4



neoplasms *see* tumors  
 neurocardiogenic stunning 227  
 nitrogen-15-labelled ammonia for PET 72  
 nuclear medicine 68-75  
 chronic CAD 193, 195  
 Nyquist limit 44



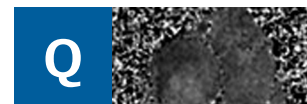
oblique views, technique 5  
 obstructive hypertrophic cardiomyopathy 215, 218, 219  
 offline reconstruction in 3D echocardiography 35-6  
 optical coherence tomography 173  
 Optison 37  
 osteosarcoma 238  
 ostium primum 141  
 ostium secundum 141  
 outflow tract  
 LV  
 Doppler studies of flow velocity 46  
 echocardiographic studies of gradient across 51  
 MRI 95  
 obstruction in hypertrophic cardiomyopathy 215, 218, 219  
 RV, MRI 97  
 output, cardiac  
 cardiac catheterization assessment 60-1  
 echocardiographic assessment 48  
 oxygen saturation measurements, catheterization methods 60  
 oxygen-15-labelled water for PET 72



pacing in dilated cardiomyopathy, echocardiographic criteria 216-17  
 pain, chest *see* chest pain  
 papillary fibroelastoma 233, 236  
 papillary muscle rupture 150, 152  
 parallel imaging  
 MR angiography of great vessels 129  
 MRI 113  
 paramagnetics in MRI *see* gadolinium  
 partial anomalous pulmonary venous drainage 261  
 partial (fractional) echo, MR angiography of great vessels 128  
 percutaneous approach to cardiac catheterization 59  
 percutaneous balloon transluminal angioplasty (PTCA) 201  
 with stent 201, 208-10  
 perfusion, myocardial 111-16  
 assessment 111-16, 186  
 in chronic CAD 191, 191-3  
 MRI 111-16, 186, 191-3  
 nuclear imaging 71, 72, 72-3  
 physiology 111-12  
*see also* reperfusion

perfusion, pulmonary, CT imaging 254  
 pericarditis 25, 26, 245-7  
 constrictive *see* constrictive pericarditis  
 pathophysiology and clinical features 25, 26, 245-6  
 pericardium 25-7, 243-51  
 anatomy 243  
 effusions *see* effusions  
 imaging modalities 243-4  
 non-neoplastic disorders 244-50, 250-1  
 tumors 232, 250  
 angiosarcoma 238-9  
 lymphangioma 238  
 mesothelioma 234, 239-40  
 metastases 240, 250  
 teratoma 238  
 PET *see* positron emission tomography  
 pharmacological stress imaging  
 in chronic CAD 188-9, 191, 193, 194, 195-6  
 echocardiography 38  
 MRI 107  
 perfusion studies 113  
 myocardial scintigraphy 68  
 phase-sensitive inversion-recovery sequences 118  
 pheochromocytoma 233, 237  
 pigtail catheter, angiography 59  
 PISA method *see* proximal isovelocity surface area  
 plain films *see* radiography  
 planimetry, aortic valve 157  
 plaque, atherosclerotic  
 aortic 277, 278  
 coronary vessels and in general  
 complicated 172-3, 175-6  
 CT angiography 84  
 FDG-PET 73-4  
 formation 171, 172, 172-3  
 intravascular ultrasound 65, 175, 177  
 other imaging methods 175-6  
 rupture 172-3, 175-6  
 rupture susceptibility of unstable/vulnerable plaques 176  
 pleural effusions 16-17  
 in aortic dissection 275-6  
 pericardial effusions vs 243  
 positional abnormalities *see* malposition  
 positron emission tomography (PET) 71-3  
 basic principles 68  
 myocardial scar 198  
 plaque imaging 73  
 positron emission tomography/CT (PET/CT), plaque 74  
 posteroanterior (frontal radiograph) 4  
 atrial enlargement, right 8  
 technique 5  
 ventricular enlargement  
 left 6-8  
 right 5-6  
 postoperative imaging, CAD 201-8  
 pressure (blood)  
 abnormal *see* hypertension; hypotension  
 gradients, echocardiographic studies 49  
 half-time, echocardiographic studies 49  
 intracardiac *see* intracardiac pressure; ventricles  
 intracoronary 65-6  
 Doppler studies 65-6, 66  
 transstenotic 66  
 pulmonary arterial *see* pulmonary arteries  
 pressure overload 11  
 causes 12  
 right-side heart failure due to 20  
 pressure wire, intracoronary 66  
 preventive cardiology (CHD prevention) 176-81  
 PROCAM (Prospective Cardiovascular Munster Heart) study and score 176, 181  
 prosthetic valves 166-9  
 proximal isovelocity surface area (PISA) method 48-9

mitral valve orifice area 153  
 mitral valve prosthesis 169  
 pseudoaneurysm of aorta 267  
 pseudocoarctation of aorta 265  
 PSIR sequences 118  
 pulmonary angiography  
 conventional 62  
 MR 130, 132-3  
 pulmonary arterial hypertension 252, 256  
 with atrial septal defect 142  
 chronic thromboembolic *see* thromboembolic pulmonary hypertension, radiography 11, 15-16, 25  
 pulmonary arteries 252-6  
 bronchial carcinoma invasion 261-2  
 disorders 252-6  
 aneurysms 262  
 embolism *see* emboli  
 sarcomas (PAS) 256, 257  
 position in atrial situs 102  
 pressure  
 echocardiographic calculation 51  
 high *see* pulmonary arterial hypertension  
 pulmonary capillary wedge pressure measurement 60  
 pulmonary non-vascular problems *see* lungs  
 pulmonary valve  
 combined disease of tricuspid and 165  
 insufficiency 165  
 MRI 110  
 MRI of normal valve 97  
 stenosis 165  
 pulmonary veins  
 disorders 260-1  
 congestion 12, 18, 21  
 sarcomas (PVS) 256, 257  
 flow velocity, Doppler studies 46  
 incompletely opacified (in CT angiography), vs pulmonary embolism 254  
 pulmonary vessels (in general) 252-63  
 angiography *see* pulmonary angiography  
 disorders 252-63  
 neoplastic 133, 256-60, 261-2  
 radiography 11-16  
 pulsation artifacts, CT angiography of great vessels 86  
 pulse sequences  
 MR angiography  
 coronary 123  
 great vessels 128-9  
 MRI 91-2  
 delayed-enhancement imaging 117-19  
 functional imaging 105  
 morphological imaging 98  
 perfusion imaging 112-13  
 pulsed Doppler 44



qualitative perfusion MRI analysis 114-15  
 quantitative perfusion MRI analysis 116



R wave, MRI and 99  
 radial artery approach to coronary angiography 63  
 radiofrequency (RF) ablation, atrial fibrillation 261  
 radiofrequency (RF) data, tracking in 47  
 radiography, conventional (plain films/X-rays) 3-33  
 anatomy 4-33

pericardial 243  
 technique 5  
 radionuclide imaging *see* scintigraphy; single-photon emission computed tomography  
 radiotracers  
 myocardial scintigraphy 69-70  
 PET 72-3  
 rate, heart, CT coronary angiography 80-1  
 regurgitant volume  
 in aortic insufficiency 158, 161  
 in aortic stenosis 155  
 echocardiographic assessment 48-9  
 in mitral valve insufficiency 150, 151, 153, 154  
 remodelling in coronary atherosclerosis 171-2  
 negative 172, 177  
 positive 172, 177  
 renal disorders, hypertension due to 24  
 renal failure, CT angiography contraindicated in 254  
 reperfusion 184  
 injury on 183, 184  
 repetition times (TR) 98  
 MR angiography of great vessels 128  
 respiratory artefacts vs pulmonary embolism (on CT angiography) 254  
 respiratory distress (dyspnea) 3  
 respiratory motion in MR coronary angiography, compensation angiography for 123-4  
 re-stenosis with coronary stents 208, 209  
 restrictive cardiomyopathies 23, 215, 221-5  
 imaging 221-2  
 radiography 23  
 resynchronization therapy in dilated cardiomyopathy, echocardiographic criteria 216-17  
 revascularization procedures 201-10  
 rhabdomyoma 233, 237  
 rhabdomyosarcoma 234, 240  
 rheumatic fever 147  
 risk factors for CHD, preventive strategies related 176-81  
 rubidium-82 for PET 72-3



saline, contrast echocardiography 37  
 sarcoidosis 222-4  
 sarcomas  
 cardiac 238-9  
 MRI signal characteristics 234  
 pulmonary vascular 256-9  
 saturation time, perfusion MRI 112  
 scar  
 myocardial *see* myocardium  
 pericardial, in constrictive pericarditis 247  
 scatter/scattering  
 broadband 34  
 integrated 34-5  
 scintigraphy, myocardial 68-71  
 myocarditis 228, 229  
 sclerosis, arterial *see* atherosclerosis  
 screening, CHD risk levels 176-81  
 semiquantitative analysis of perfusion MRI images 115  
 septum  
 atrial *see* atrium  
 cardiac catheterization across 59  
 ventricular *see* ventricles, septal defect  
 sestamibi 69, 70  
 shock, cardiogenic, causes 13  
 short-axis views (MRI) 92-4  
 shunts  
 intracardiac  
 angiographic detection 61  
 echocardiographic studies of flow 49  
 MRI studies 110

pulmonary arteriovenous 260  
 signal-to-noise (SNR) ratio in MRI 91  
 MR angiography of great vessels 128  
 myocardial perfusion studies 112  
 signs and symptoms of heart disease 3-4  
 single-photon emission computed tomography (SPECT)  
 basic principles 68  
 hibernating myocardium 195  
 myocardial 68-9  
 single-shot IR-SFFP sequences 118-19  
 single-shot turbo spin-echo (TSE) sequences 100  
 coronary bypass 204  
 single-slice image acquisition 77  
 sinus of Valsalva, aneurysm 242  
 sinus rhythm for CT coronary angiography 80-1  
 sinus venosus 141  
 situs ambiguus 102  
 situs inversus *see* inversion  
 size (incl. diameter), cardiac  
 echocardiographic determination 42  
 LV 51  
 radiographic determination 10  
 small-disk summation method 199  
 software, MR angiography of great vessels 128  
 Sonos method 63  
 SonoVue 37  
 SPAMM 107  
 spatial modulation of magnetization (SPAMM) 107  
 speckle tracking 47, 47-8  
 SPECT *see* single-photon emission computed tomography  
 spin-echo (SE) sequences 92  
 coronary bypass 204  
 morphological imaging 98  
 spiral (helical) CT  
 great vessels 84  
 multislice *see* multislice spiral CT  
 spoiled sequences, great vessels 128  
 SSFP *see* steady-state free precession  
 Stanford classification of aortic dissection 30, 271, 272  
 steady-state free precession (SSFP) sequence 100  
 cine *see* cine steady-state free precession  
 of coronary bypass 203-4  
 coronary MR angiography 125  
 functional imaging 106-7  
 morphological imaging 96, 100  
 single-shot IR- 118-19  
 steal phenomenon, coronary bypass graft stenosis 206  
 stenosis  
 coronary 200-1  
 CT angiography 83  
 differential diagnosis 200-1  
 Doppler studies 65, 66  
 myocardial scintigraphy 70  
 coronary bypass graft 201, 202, 203, 205, 206, 207, 208  
 pulmonary vein, complicating catheter ablation in atrial fibrillation 261  
 valvular, MRI 110  
*see also specific valves*  
 vascular (in general), MRI 110  
*see also re-stenosis*  
 stent, coronary 201, 208-10  
 stent-graft, aortic, intravascular ultrasound for implantation of 65  
 stethoscope, ultrasound 36  
 strain rate imaging 47  
 chronic CAD 190, 195  
 stress cardiomyopathy 227  
 stress imaging  
 in chronic CAD 188, 188-9, 189-90, 191, 193, 194, 195-6  
 echocardiography 38  
 wall-motion abnormalities 53, 54

MRI 107  
 perfusion studies 113  
 myocardial scintigraphy 68, 70  
 stress-strain relationships, tissue Doppler imaging 46, 53-4  
 stroke volume, echocardiographic assessment 48  
 subclavian artery, aberrant right 264  
 subendocardial vs transmural infarction or scar 196, 197  
 surgery  
 pulmonary vascular tumors 259  
 ventricular aneurysm 199  
 Svensson classification of aortic dissection 271, 272-80  
 class 1 272-6  
 class 2 277  
 class 3 277  
 class 4 278-9  
 class 5 279-80  
 symptoms and signs of heart disease 3-4  
 synchrotron radiation, atherosclerosis 174, 177  
 syncope 4  
 syndrome X 200-1  
 syphilitic aortitis 280  
 systole  
 cardiac function in, echocardiographic assessment 52  
 pulmonary arterial pressure in, echocardiographic calculation 51



T1-weighted images 98  
 T2-weighted images 98  
 tachycardias 3-4  
 Takayasu arteritis 280  
 Tako Tsubo cardiomyopathy 227  
 tamponade, pericardial, in pericarditis 245-6, 246, 247  
 technetium-99m-labelled tracer (sestamibi) 69, 70  
 Tei index 52  
 teratoma 233, 238  
 tetrafosmin 70  
 thallium chloride 69  
 thermomodulation methods, cardiac output measurement 60-1  
 thermography, atherosclerotic plaque 176  
 thoracic aortic aneurysm 30  
 three-chamber views (MRI) 95  
 three-dimensional echocardiography 35-6  
 atrial volume, left 43  
 ventricular wall motion studies 53  
 three-dimensional MR angiography of great vessels 128, 130  
 thromboembolic pulmonary hypertension, chronic 255-6  
 CT angiography 86  
 MR angiography 133  
 thrombosis  
 intracardiac 240-1  
 ventricular 200  
 plaque 172, 173, 175  
 venous, leading to pulmonary embolism 252  
 tilting-disk valves 166, 168  
 time-delayed excitation 34  
 time-resolved contrast-enhanced MRA 130  
 tissue Doppler echocardiography 45  
 in chronic CAD 190, 195  
 mitral insufficiency 153  
 prosthetic valves 169  
 reference values 46-7  
 ventricular wall-motion studies 53-4  
 total anomalous pulmonary venous drainage 260-1

tracers  
 in FDG-PET 72-3  
 radioactive *see* radiotracers

tracking in RF data (strain rate imaging) 47

transesophageal echocardiography 39, 40-1

transfemoral approach to catheterization *see* femoral artery catheterization

transmural vs subendocardial infarction or scar 196, 197

transposition of great vessels 102

transseptal cardiac catheterization 59

transthoracic echocardiography 40

transvalvular flow velocity, Doppler studies 46, 47

traumatic aortic injury/rupture 279-80  
 CT angiography 87  
 radiography 30

tricuspid valve  
 combined disease of pulmonary and 165  
 insufficiency 163-4  
 MRI 96, 97  
 stenosis 162-3  
 systolic regurgitant jet across 50

tumors  
 cardiac 232-42, 250  
 benign 232  
 diagnostic techniques 233  
 malignant *see* malignant tumors  
 pulmonary vascular 133, 256-60, 261-2

turbo (fast) spin-echo (TSE/FSE) sequences 92, 98-100  
 morphological imaging 98, 98-100  
 single-shot *see* single-shot turbo spin-echo

two-chamber view (MRI) 95

two-dimensional echocardiography 35  
 LV function 52  
 quantification using 42-3

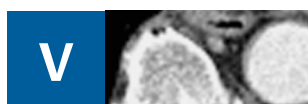


Uhl anomaly 226

ulcers (atheromatous plaque-associated)  
 aorta 278-9  
 coronary arteries 172

ultrasound  
 basic principles 35-6  
 cardiac *see* echocardiography  
 intravascular *see* intravascular ultrasound

ultrasound stethoscope 36



Valsalva's sinus, aneurysm 242

valves (cardiac) 141-69  
 acquired disease 141-69  
 vegetations 234

Doppler studies of flow velocity across 46

echocardiographic assessment  
 orifice area 49  
 regurgitant volume 48-9  
 MRI 96-7  
 insufficiency and stenosis 110  
 prosthetic 166-9  
*see also specific valves*

vascular anomalies, congenital *see* congenital cardiovascular anomalies

vasodilation induction in echocardiography 38

vasospastic angina pectoris 201

vegetations, valvular 234

venous congestion, pulmonary 12, 18, 21

venous grafts for coronary bypass 201, 203

venous thrombosis leading to pulmonary embolism 252

ventricles  
 aneurysms 198-200  
 angiography  
 LV 61  
 RV 61  
 arrhythmogenic RV dysplasia/cardiomyopathy *see* arrhythmogenic RV dysplasia/cardiomyopathy  
 enlargement/dilatations  
 LV 6-8, 11  
 radiographs 5-8  
 RV 5-6  
 function, echocardiographic assessment 51-6  
 LV 51-2  
 LV, in aortic dissection 275  
 RV 52-3  
 function, MRI assessment in chronic CAD 191  
 hypertrophy 11  
 inflow tract *see* inflow tract  
 isolated non-compaction of LV 227  
 motion *see* motion  
 MRI  
 of anomalies 102, 103  
 LV 94, 95  
 RV 96, 97  
 muscle mass, LV, echocardiographic estimation 41  
 nuclear imaging of LV 68, 72, 73  
 outflow tract *see* outflow tract  
 pressure, LV  
 echocardiographic studies of filling pressure 50, 55-6  
 echocardiographic studies of rise and fall 52  
 pressure, RV, echocardiographic studies 50, 51  
 pressure and/or volume overload  
 LV 11  
 RV 12  
 septal defect 144-6  
 echocardiographic studies 50-1, 145  
 thrombosis 200  
 volume *see* volume  
 wall *see* wall

vertical long axis (MRI)  
 LV 95  
 RV 96

viral infections, myocardial 228, 229

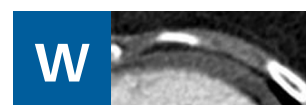
virtual histology, atherosclerotic plaque 175-6

visual analysis of perfusion MRI images 114-15

volume, chambers  
 echocardiographic estimation  
 LA 43, 43  
 LV 41, 43  
 RV 43  
 MRI, ventricles 104  
*see also* regurgitant volume; stroke volume

volume calcium score 77

volume overload 11  
 causes 12  
 heart failure due to 20  
 volume rendering technique 82  
 coronary bypass 202, 204



wall  
 aortic, increased tension causing dissection 272  
 cardiac/myocardial/ventricular motion *see* motion  
 thickness determination 195

water, <sup>15</sup>O-labelled, for PET 72

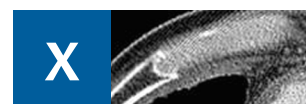
WHO classification of cardiomyopathies 22-3, 215

whole-heart MR coronary angiography 121

Williams-Bueren syndrome 264

women with coronary heart disease, myocardial scintigraphy 71

World Health Organization of cardiomyopathies 22-3, 215



X-rays  
 in CT 80  
 for plain films *see* radiography



zero filling, MR angiography of great vessels 128-9